Dynamic scaling and freezing criteria in quasi-two-dimensional dispersions

Raphaël Pesché
Department of Chemical Engineering, University of Delaware, Newark, Delaware 19716

Markus Kollmann and Gerhard Nägele*
Institut für Festkörperforschung, Teilinstitut 4: Weiche Materie, Forschungszentrum Jülich, D-52425 Jülich, Germany
(Received 13 April 2001; published 22 October 2001)

We report on a Brownian dynamics simulation study of quasi-two-dimensional dispersions of colloidal spheres interacting by long-range electrostatic and dipolar magnetic forces. The calculated dynamic correlation functions are shown to obey dynamic scaling in terms of a characteristic relaxation time related to the mean particle distance and, due to hydrodynamic interactions, to the particle size. The dynamical freezing criterion of Löwen [Phys. Rev. E **53**, R29 (1996)] is shown to be equivalent to a two-dimensional static freezing criterion.

DOI: 10.1103/PhysRevE.64.052401 PACS number(s): 82.70.Dd, 05.10.Gg, 05.40.Jc

There has been strong interest in recent years in the static and dynamic properties of quasi-two-dimensional (Q2D) dispersions of spherical colloidal particles. Well-studied examples of such dispersions are charged particles confined between two narrow glass plates [1,2], and superparamagnetic particles close to a water-air interface and interacting via repulsive dipolar magnetic forces [3]. Part of the interest in these systems arises from the fact that, contrary to low-molecular liquids, the range and strength of the particle interactions can be experimentally controlled. Moreover, the particle trajectories can be directly tracked using video microscopy imaging [1]. One area of intensive research is concerned with the nature of two-dimensional freezing and melting that, contrary to three-dimensional systems, can be a two-stage process of continuous phase transitions with an intermediate hexatic phase [3].

This report is concerned with the general dynamic behavior of Q2D dispersions of spherical particles with strong and long-range repulsive interactions. The dynamics of colloidal dispersions is controlled not only by direct interparticle forces, but also by solvent-mediated hydrodynamic interactions (HI), which can lead to remarkable dynamical effects [4,5]. We employ a Brownian dynamics (BD) simulation method to analyze the static and dynamic scaling behavior of these Q2D systems, and to study its implication on related static and dynamic freezing criteria. For the first time, particular focus is given to reveal the influence of HI on dynamic scaling and on a related dynamic freezing criterion.

Two types of effective pair potentials are considered: first a two-dimensional Yukawa potential [6]

$$\beta u(r) = L_B Z^2 \frac{e^{-\kappa r}}{r}, \quad r > \sigma \tag{1}$$

with a hard core part for $r<\sigma$, where r is the distance between two charged spheres of diameter $\sigma = 2a$, Z is an effective particle charge in units of the elementary charge, $\beta = 1/k_B T$, and L_B is the so-called Bjerrum length of the solvent. Equation (1) has been used in various simulation studies as a model potential for the lateral interaction of charged colloidal spheres between two close planar glass plates, with the screening length κ^{-1} determined by the counterions dissociated from the plates [5,7]. The second potential is of dipolar form

$$\beta u(r) = \frac{\mu_0}{4\pi k_B T} \frac{M^2}{r^3}, \tag{2}$$

and describes to very good accuracy the magnetic repulsion of superparamagnetic colloidal spheres of induced magnetic moment $M = \chi_{\text{eff}} B$ located at a liquid-air interface, with a magnetic field of strength B applied perpendicular to the interface. Here, χ_{eff} is the effective magnetic particle susceptibility. Such well-defined Q2D systems have been studied in [8,9].

The BD finite difference equation employed here for the trajectories of N Brownian spheres in a fluid of viscosity η reads [5,9]

$$\Delta \mathbf{R}_i = \sum_{j=1}^{N} [\beta \mathbf{D}_{ij}(\mathbf{R}^N) \cdot \mathbf{F}_j^P + \nabla_j \cdot \mathbf{D}_{ij}(\mathbf{R}^N)] \Delta t + \Delta \mathbf{X}_i + O(\Delta t^2), \tag{3}$$

where $\Delta \mathbf{R}_i$ is a two-dimensional vector describing the in-plane displacement of particle i during time t to $t+\Delta t$, $\mathbf{F}_j^P$ is the direct force on particle j at t derived from the pair potentials of Eqs. (1) and (2), respectively, and $\mathbf{D}_{ij}(\mathbf{R}^N)$ is the hydrodynamic diffusivity tensor. The latter depends in principle on the configuration $\mathbf{R}^N = \{\mathbf{R}_1, \ldots, \mathbf{R}_N\}$ of all N spheres at time t and accounts for the solvent-mediated HI between particles i and j. The two-dimensional vector $\Delta \mathbf{X}_i$ is a Gaussian-distributed random displacement with zero mean

*Corresponding author. Electronic address: g.naegele@fz-juelich.de

TABLE I. Parameters of the Q2D superparamagnetic aqueous system I and charged systems II and III without HI, and with pair potentials in Eqs. (1) and (2), respectively. The Bjerrum length, $L_B = 7.2$ Å, corresponds to water as solvent at room temperature. The coupling parameters are $\Gamma_I = \beta\mu_0 M^2 n^{3/2}/(4\pi)$ and $\Gamma_{\mathrm{II,III}} = L_B Z^2 n^{1/2}$.

	System I	System II	System III
$C = \pi n a^2$	0.02	0.01	0.003
r_0/a	12.5	17.7	32.4
Γ	3.9	47.8	91.4
$k = \kappa r_0$		2.5	3.9
r_m/r_0	0.98	0.98	0.97
$-\beta r_0\, du/dr\|_{r=\kappa^{-1}}$		112	420

and covariance matrix $\langle \Delta\mathbf{X}_i \Delta\mathbf{X}_j \rangle = 2\mathbf{D}_{ij}\Delta t$, where the brackets indicate an equilibrium ensemble average. We employ a time step Δt within the range of 10^{-5}–10^{-4} τ_0, where $\tau_0 = 1/(nD_0)$ is the time needed for a particle to diffuse the geometrical interparticle distance $r_0 = n^{-1/2}$. Here, n is the two-dimensional number density, and D_0 is the free diffusion coefficient of a particle. For the strongly repelling and rather dilute systems under consideration, HI are dominated by their pairwise additive long-range part. We therefore treat $\mathbf{D}_{ij}$ to good accuracy within the Rotne-Prager level, which preserves the positive definiteness of the exact diffusivity tensor matrix. The long-range nature of HI is accounted for by employing an Ewald-like summation technique. The influence of HI on dynamic properties is analyzed by comparison with BD calculations with HI disregarded.

Three systems I–III are analyzed, with parameters listed in Table I. System I is an aqueous magnetic system described by the pair potential (2), whereas systems II and III are aqueous charge-stabilized dispersions characterized by the pair potential (1). These systems are examples of strongly repulsive particle dispersions with pronounced next neighbor shells and masked excluded volume interactions, characterized in their static behavior by a single length scale given by r_0. The radial distribution function $g(r)$ of these systems reveals a pronounced principal peak located at a radial distance r_m (cf. BD results in Fig. 1 and Table I), nearly equal to r_0. The system parameters are such that the three $g(r)$'s have the same principal peak height $g(r_m)$. When plotted vs reduced distance $x = r/r_0$, the $g(r)$'s are seen from the inset of Fig. 1 to superimpose nearly perfectly within the x range depicted. This static scaling behavior implies that the corresponding two-dimensional static structure factors $S(q) = 1 + 2\pi n \int_0^\infty dr\, r[g(r)-1]J_0(qr)$ of systems I–III, where q is the scattering wave number and J_0 the zeroth-order Bessel function of the first kind, nearly coincide when plotted vs the reduced wave number $y = q/q_0$. Here, $q_0 = 2\pi/r_0 \approx q_m$ with the peak of $S(q)$ located at q_m.

Provided that $r_m \approx r_0$ is the only relevant length scale also for the particle dynamics, as expected without HI, there is a single characteristic time scale $\tau_0 = r_0^2/D_0$ associated with r_0. Dynamic properties like the dimensionless distinct van Hove correlation function $g_d(r,t) = n^{-1}\langle \sum_{i\neq j=1}^{N} \delta(\mathbf{r} - \mathbf{R}_i(t) + \mathbf{R}_j(0))\rangle/N$ and the lateral mean-squared displacement $W(t) = \langle [\mathbf{R}_i(t) - \mathbf{R}_i(0)]^2 \rangle/4$ depend on r and t only through x and the reduced time $\tau = t/\tau_0$. The function $g_d(r,t)$ is proportional to the conditional probability density of finding, at time t, a particle a distance r apart from the location of another one at $t = 0$. Since $g_d(r,0) = g(r)$, $g_d(r,t)$ is the time-dependent generalization of $g(r)$. Quantities like $g_d(r,t)$ and $W(t)$ can be measured using colloidal video imaging. BD results without HI for the $g_d(r,t)$'s of I–III at time $t = 0.032\tau_0$ are shown in Fig. 1. Corresponding results for the

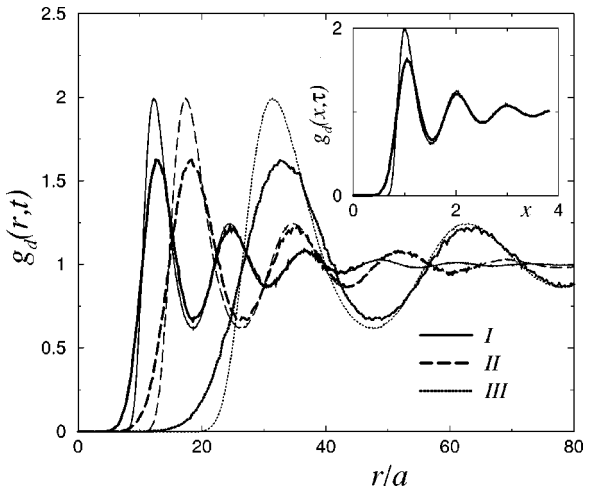

FIG. 1. BD results without HI for the distinct van Hove function $g_d(r,t)$ of systems I–III (cf. Table I) at $t = 0$ (thin lines), where $g_d(r,0) = g(r)$, and at $t/\tau_0 = 0.032$ (thick lines). The characteristic times τ_0 of I–III are different from each other. Inset: $g_d(x,\tau)$ vs dimensionless distance $x = r/r_0$ and reduced time $\tau = t/\tau_0$, with $r_0 = n^{-1/2}$ and $\tau_0 = (nD_0)^{-1}$.

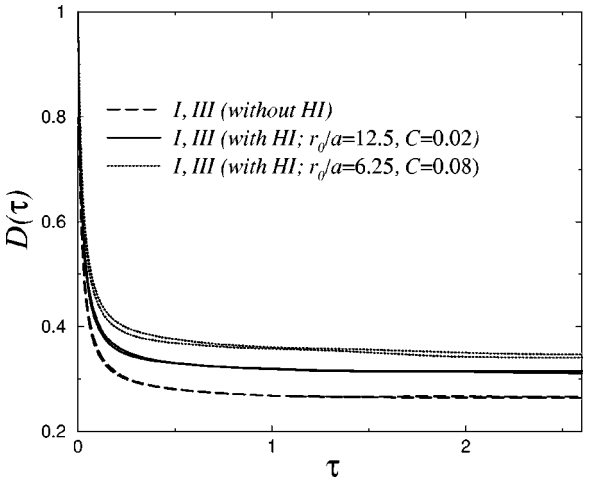

FIG. 2. Normalized self-diffusion function $D(t) = W(t)/(tD_0)$ of systems I and III with/without HI vs reduced time τ. With HI, the system parameters are as in Table I, aside from r_0/a and surface fraction C that are given in the figure. For fixed potential parameters and fixed r_0, we consider $r_0/a = 12.5$ and 6.25, with $S(q_m) = 2.3$. Without HI, the long-time asymptotic value is given by $D(\infty) \approx 0.26$. With HI, $D(\infty) \approx 0.31$ for $r_0/a = 12.5$, and $D(\infty) \approx 0.34$ for $r_0/a = 6.25$.

normalized reduced self-diffusion function $D(t) = W(t)/(D_0 t)$, with $D(0)=1$, vs reduced time τ are shown with/without HI in Fig. 2. The inset in Fig. 1 clearly demonstrates dynamic scaling, according to which colloidal systems with long-range repulsion and identical peak heights $g(r_m)$ [likewise, identical $S(q_m)$] have nearly identical dynamic properties, e.g., identical $g_d(r,t)$ and $W(t)/r_m^2$, as functions of reduced distance and time. The correlation time $t/\tau_0 = 0.032$ corresponds to $t \approx 5\tau_a$ for I, $t \approx 10\tau_a$ for II, and $t \approx 34\tau_a$ for III, where $\tau_a = a^2/D_0$. As seen from Fig. 2, this time lies in the intermediate time regime where the reduced mean-squared displacement $D(t)$ has approached the asymptotic long-time value $D(\infty)$ (cf. caption of Fig. 2).

Although the dynamic scaling appears reasonable for systems characterized by a single relevant static length scale, it is by no means a trivial result. Dynamic scaling of the dynamic structure factor $S(q,t)$ related to $g_d(r,t)$ by Fourier transformation, as function of reduced wave number y and time τ, has been predicted very recently for three-dimensional deionized charge-stabilized suspensions using a mode coupling approximation (MCA) with HI neglected [10]. While the dynamic scaling predictions of the MCA apply also to q-space dynamic properties in two dimensions, the present Q2D simulation study provides an unambiguous validation of dynamic scaling, particularly regarding the involved approximations made in the MCA. Note that the dipolar potential provides no characteristic length whereas the Yukawa potential includes κ^{-1} as an intrinsic length. The screening lengths κ^{-1} of the charged systems II and III are significantly smaller than r_m (cf. Table I) and, since $r_0 \beta\, du/dr|_{r=\kappa^{-1}} \gg 1$ with pronounced next neighbor shells at distance r_0, are therefore of no relevance regarding scaling.

The potentials (1) and (2) are special cases of the form $\beta u(r) = A r^{-l} f(\kappa r)$ with regular function f, amplitude A, and exponent l. By expressing Eq. (3) without HI, and the Ornstein-Zernicke equation associated with $g(r)$ [11], in terms of reduced position vectors $\mathbf{R}_i/r_0$ and reduced time τ, one can see that systems of equal dimensionless coupling parameter $\Gamma = A n^{l/2}$ and reduced screening parameter $k = \kappa n^{-1/2}$ are statically and dynamically equivalent. According to Table I, the employed values for Γ and for k are all different from each other. This shows that the dynamic scaling is not just a straightforward consequence of the forms of potentials (1) and (2). Since $c(x) \approx -\beta u(x) = -\Gamma f(kx)/x^l$ for very large separations $r \gg r_0$, with $c(x)$ denoting the direct static correlation function [11], there are differences in the small wave number behavior of $S(y)$ for systems I–III, and thus in their thermodynamic properties. However, these differences are visible only when $n\hat{c}(y) = 1 - 1/S(y)$ is plotted instead of $S(y)$, where $\hat{c}(y)$ is the Fourier transform of $c(y)$ [10,11].

The dynamic scaling for Q2D dispersions with strong and long-range particle repulsions implies that systems with equal $g(r_m)$ [and $S(q_m)$] also have the same value of the normalized long-time self-diffusion coefficient $D_S^L = \lim_{t\to\infty} W(t)/t$. The one-to-one correspondence between $S(q_m)$ and D_S^L/D_0 is shown in Fig. 3, with D_S^L extrapolated

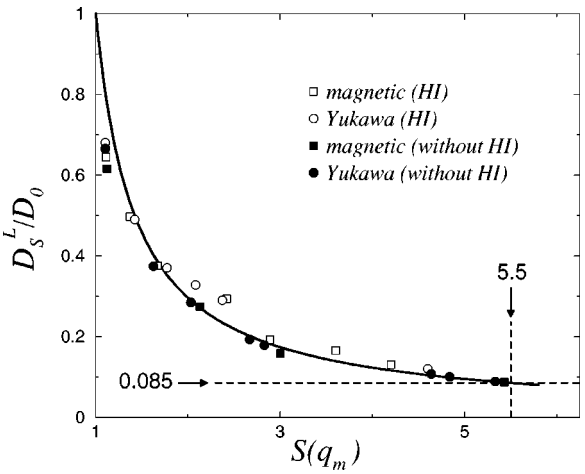

FIG. 3. Reduced long-time self-diffusion coefficient D_S^L/D_0 without HI and with HI (for fixed ratio $r_0/a = 6.25$) vs structure factor peak height $S(q_m)$. System parameters as for I and III, aside from Γ and k, which are varied (through κ, Z, n, and B). Solid line: parametrization of the relation $D_S^L/D_0 = f(S(q_m))$, using the form $f(z) = 0.42/(z - 0.58)$ with $f(1)=1$ and $f(5.5)=0.085$ that holds approximately for $z \geq 1.5$.

from large-t BD calculations of $W(t)$ as described in Ref. [12]. Without HI, our long-time results for D_S^L/D_0 vs $S(q_m)$ of the magnetic and Yukawa systems are located on a single master curve (cf. Fig. 3), in particular with a value of $D_S^L/D_0 \approx 0.085$ for $S(q_m) \approx 5.5$. According to an empirical dynamical criterion for two-dimensional freezing found by Löwen [12] from BD simulations without HI for various inverse-power pair potentials, $D_S^L/D_0 \approx 0.085$ at the freezing line independent of $u(r)$ and the nature of the freezing process. Moreover, the peak height $S(q_m)$ of the liquid static structure factor at two-dimensional freezing was found to be about 5.5 [13] at the freezing line, in good accord with the BD results of Fig. 3. For comparison, the three-dimensional Hansen-Verlet rule [14] of freezing gives a smaller value for $S(q_m)$ of about 2.85. This indicates the more strongly pronounced static correlations in two-dimensional fluids close to freezing. In contrast, the value of $D_S^L/D_0 \approx 0.098$ for three-dimensional freezing [10,12] is rather close to the one in two dimensions. A freezing value of $D_S^L/D_0 \approx 0.1$ was obtained for three-dimensional hard-sphere dispersions also by Fuchs [15] using mode-coupling theory asymptotic laws without HI. The work of Fuchs corrects earlier work of Indrani and Ramaswamy [16] who attempted to relate the Hansen-Verlet freezing rule to the one of Löwen *et al.* using simplified mode-coupling ideas. With the scheme of Indrani and Ramaswamy, the observed freezing value $D_S^L/D_0 \approx 0.1$ has been underestimated by a factor of 2. Summarizing, we have shown that the equivalence of two seemingly unrelated static [13] and dynamic [12] criteria for two-dimensional freezing is a consequence of dynamic scaling.

So far we have disregarded the dynamical influence of HI, which introduces the particle radius a as another relevant length scale. For the pairwise-additive far-field part of the hydrodynamic diffusivity tensor prevailing for the systems under consideration, this fact becomes apparent from

$\mathbf{D}_{ij}(\mathbf{R}^N)/D_0 \approx \mathbf{D}_{ij}^{(2)}([\mathbf{R}_i - \mathbf{R}_j]/a)/D_0$, where $\mathbf{D}_{ij}^{(2)}$ is the pairwise additive two-body part of $\mathbf{D}_{ij}$ [17]. With HI, there exists thus a more restricted form of dynamic scaling where the master curves for $g_d(x,\tau)$ and $D(\tau)$ depend on a/r_0. This restricted scaling can be deduced also from MCA results for Brownian systems with far-field HI included [18].

BD results for $D(\tau)$ and D_S^L/D_0 vs. $S(q_m)$ with HI are depicted in Figs. 2 and 3 for magnetic and Yukawa systems. In Fig. 2, two size ratios $r_0/a = 6.25$ and 12.5 are used to show the dependence of $D(\tau)$ on r_0/a. The observed modest enhancement of self-diffusion is indicative of prevailing far-field HI [5,8,9,18]. The BD results of $D(\tau)$ for I and III with HI and given a/r_0 are seen, aside from statistical uncertainties, to be nearly identical with each other. According to Fig. 2, the enhancement of $D(\tau)$ is smaller for smaller a/r_0. The value of D_S^L/D_0 close to freezing is thus only modestly enlarged by HI as anticipated from Fig. 3 for the case $r_0/a = 6.25$. BD simulations with HI become exceedingly time consuming when the freezing point is approached, since a large number of particles is needed to account for strong and long-range particle correlations. Note that the short-time self-diffusion coefficient $D_S^S = \lim_{t\to 0} W(t)/t$ is equal to D_0 for systems with prevailing far-field HI. For systems with dominating near-field HI and strong lubrication forces, like dispersions of colloidal hard spheres, $D_S^S < D_0$ and the dynamic freezing criterion must then be stated in terms of D_S^L/D_S^S instead of D_S^L/D_0, as shown for three-dimensional bulk systems by experiment [19] and by rescaled MCA calculations [10].

To conclude, we have analyzed the static and dynamic scaling behavior of strongly repulsive Q2D dispersions with and without HI. Dynamic scaling was shown for these systems to be at the origin of the equivalence of two freezing criteria for the onset of two-dimensional freezing. Further extensions of this work will address possible consequences of dynamic scaling on higher order static and dynamic correlation functions with more than two particle coordinates involved, and possible connections with a corresponding states relationship for transport coefficients introduced by Rosenfeld [20].

We acknowledge very helpful support in part of the BD simulation coding by B. Rinn and P. Maass, and we thank R. Klein and J. K. G. Dhont for their interest and the Deutsche Forschungsgemeinschaft (SFB 513) for funding.

[1] H. Acuña-Campa, M.D. Carbajal-Tinoco, J.L. Arauz-Lara, and M. Medina-Noyola, Phys. Rev. Lett. **80**, 5802 (1998).
[2] A.E. Larsen and D.G. Grier, Nature (London) **385**, 230 (1997).
[3] K. Zahn and G. Maret, Phys. Rev. Lett. **85**, 3656 (2000).
[4] T.M. Squires and M.P. Brenner, Phys. Rev. Lett. **85**, 4976 (2000).
[5] R. Pesché and G. Nägele, Europhys. Lett. **51**, 584 (2000); Phys. Rev. E **62**, 5432 (2000).
[6] E. Chang and D.W. Hone, Europhys. Lett. **5**, 635 (1988).
[7] H. Löwen, J. Phys.: Condens. Matter **4**, 10 105 (1992).
[8] K. Zahn, J.M. Méndez-Alcaraz, and G. Maret, Phys. Rev. Lett. **79**, 175 (1997).
[9] B. Rinn, K. Zahn, P. Maass, and G. Maret, Europhys. Lett. **46**, 537 (1999).
[10] A.J. Banchio, G. Nägele, and J. Bergenholtz, J. Chem. Phys. **113**, 3381 (2000).
[11] J. P. Hansen and I. R. McDonald, *Theory of Simple Liquids* (Academic Press, New York, 1986).
[12] H. Löwen, Phys. Rev. E **53**, R29 (1996).
[13] J.Q. Broughton, G.H. Gilmer, and Y.D. Weeks, Phys. Rev. B **25**, 4651 (1982).
[14] J.P. Hansen and L. Verlet, Phys. Rev. **184**, 151 (1969).
[15] M. Fuchs, Phys. Rev. Lett. **74**, 1490 (1995).
[16] A.V. Indrani and S. Ramaswamy, Phys. Rev. Lett. **73**, 360 (1994).
[17] S. Kim and S.J. Karrila, *Microhydrodynamics: Principles and Selected Applications* (Butterworth-Heinemann, Boston, 1991).
[18] G. Nägele and P. Baur, Physica A **245**, 297 (1997); Europhys. Lett. **38**, 557 (1997).
[19] H. Löwen, T. Palberg, and R.G. Simon, Phys. Rev. Lett. **70**, 1557 (1993).
[20] Y. Rosenfeld, Phys. Rev. E **62**, 7524 (2000).